

Repurposing of Fruit Peel Waste as a Green Reductant for Recycling of Spent Lithium-Ion Batteries

Zhuoran Wu, Tanto Soh, Jun Jie Chan, Shize Meng, Daniel Meyer, Madhavi Srinivasan,* and Chor Yong Tay*



Cite This: *Environ. Sci. Technol.* 2020, 54, 9681–9692



Read Online

ACCESS |



Metrics & More



Article Recommendations



Supporting Information

ABSTRACT: The development of environmentally benign hydrometallurgical processes to treat spent lithium-ion batteries (LIBs) is a critical aspect of the electronic-waste circular economy. Herein, as an alternative to the highly explosive H_2O_2 , discarded orange peel powder (OP) is valorized as a green reductant for the leaching of industrially produced LIBs scraps in citric acid (H_3Cit) lixiviant. The reductive potential of the cellulose- and antioxidant-rich OP was validated using the 3,5-dinitrosalicylic acid and 2,2'-azino-bis(3-ethylbenzothiazoline-6-sulfonic) acid assays. Leaching parameters such as OP concentration (200 mg), processing temperature (100 °C), H_3Cit concentration (1.5 M), reaction duration (4 h), and slurry density (25 g/mL) were systematically optimized to achieve 80–99% leaching efficiencies of Ni, Mn, Co, and Li from the LIB “black mass”. Importantly, solid side-streams generated by the OP-enabled leaching displayed negligible cytotoxicity in three different human cell lines, suggesting that the process is environmentally safe. As a proof of concept, $Co(OH)_2$ was selectively recovered from the green lixiviant and subsequently utilized to fabricate new batches of $LiCoO_2$ (LCO) coin cell batteries. Galvanostatic charge–discharge test revealed that the regenerated batteries exhibited initial charge and discharge values of 120 and 103 mAh/g, respectively, which is comparable to the performance of commercial LCO batteries. The use of fruit peel waste to recover valuable metals from spent LIBs is an effective, ecofriendly, and sustainable strategy to minimize the environmental footprint of both waste types.



INTRODUCTION

Lithium-ion batteries (LIBs) are currently used in a wide range of electronic products (e.g., smartphones, notebooks, cameras, electronic vehicles, medical devices, etc.) and have become an indispensable part of our daily life.^{1,2} According to a recent report, the global market value of LIBs is expected to reach a staggering \$139 billion by 2026.³ As the demand for LIBs continue to grow at a rapid pace,⁴ so does the pile of spent LIB waste. However, only 2% and 5% of the LIB waste are currently recycled per annum in Australia and EU, respectively.^{5,6} The majority of the spent LIBs often end up in landfills or incinerators, which are both environmentally unfriendly and economically unwise.^{6,7}

LIB waste contains numerous valuable resources like cobalt (Co), lithium (Li), and other metals that could be recovered and reused. In fact, out of the \$23.51 billion worth of the LIBs that are annually produced, most of the value stems from the metallic constituents.⁸ Current methods to recycle LIBs include pyro-, bio-, and hydrometallurgy. Pyrometallurgy refers to the thermal treatment of the LIB waste at extremely high temperature (>500 °C) to smelt the valuable metals. Although this process is widely used in industry, it is characteristically energy-intensive and emits a substantial level of hazardous

toxic gas.⁹ Comparatively, the use of acid-generating microbes (bacteria/fungi) such as *Acidithiobacillus ferrooxidans*, *Acidithiobacillus thiooxidans*, and *Aspergillus niger* to extract heavy metals from the LIB waste in biometallurgy exerts minimal environmental and health impacts.^{10–12} However, the industrial adoption of this process is severely curtailed due to the inefficiency of the bioleaching process and the susceptibility of the microbes to the toxic effects of the metals.¹³ In contrast, hydrometallurgy, which makes use of water as a solvent, provides a more direct metal recovery route. In terms of the operational conditions, the processing temperatures in hydrometallurgy (10 to 200 °C)¹⁴ are significantly lower than pyrometallurgy and its efficiency is independent of the growth kinetics of the microbes. Additionally, the low energy consumption, high recovery rate, and ease

Received: May 7, 2020

Revised: June 27, 2020

Accepted: July 9, 2020

Published: July 9, 2020



of operation associated with hydrometallurgy make it a highly attractive approach to treat LIB waste.

Conventional hydrometallurgical processes rely heavily on the combinatorial use of strong inorganic acids (e.g., H_2SO_4 , HCl , and HNO_3) and reductants (e.g., H_2O_2) to leach out metals from spent cathode materials.¹⁵ However, the industrial-scale utilization of strong acids will generate a substantial amount of secondary pollutants such as SO_3 , Cl_2 , and NO_x , which may pose significant potential safety and health risks. Therefore, several studies have started to explore the use of less hazardous weak organic acids such as formic, salicylic, citric, gluconic, itaconic, succinic, and acetic acids to replace the strong acids.^{16–18} When combined with H_2O_2 as the reducing agent, these mild organic acids can be as effective as mineral acids and also environmentally safe. For instance, leaching efficiencies of Li and Co from discarded LiCoO_2 (LCO) in citric acid (H_3Cit) (1.25 M) was reported to increase from 54% to 99% and 25% to 91%, respectively, when H_2O_2 (1.0 vol %) was added to the lixiviant.¹⁹ At an optimized combination of tartaric acid (0.6 mol/L) and H_2O_2 (3 vol %), selective leaching of Li (99.1%) can be achieved from cathode materials of spent LIBs. Additionally, tartaric acid can also concomitantly function as a precipitation agent for the recovery of cobalt tartrate with purity of 96.4%.²⁰ While the effectiveness of H_2O_2 as a reducing agent is undisputed, its long-term reliance is hardly sustainable since H_2O_2 is highly explosive, hazardous, and unstable.²¹ Thus, the search for greener alternatives to H_2O_2 has gained significant traction in recent years. Experiments using alternative inorganic reductants such as sodium thiosulfate²² and sodium bisulfite (NaHSO_3)²³ have shown that conditions can be optimized to achieve 80–90% leaching efficiencies of Li and Co from spent LIB cathode materials. Nonetheless, the introduction of Na^+ to the lixiviant may contaminate the final recovered products and incur additional operational cost for downstream product purification steps.

Recently, there is an outburst of interest to valorize organic waste residues produced along the food supply for various applications.²⁴ The total amount of food waste generated in the EU was estimated to be 123 kg/person/year, of which fruit and vegetable waste (FVW) accounted for about 60%.²⁵ Most of the FVW either gets burnt or is disposed off in landfills.²⁶ Not only is the current practice of dealing with FVW unsustainable but also represents a huge wastage of critical resources. Noting that FVW is rich in a plethora of redox-active molecules, such as dietary fibers, catechins, phenolic acids, and flavonoids,²⁷ researchers have begun to explore the possible use of this class of “waste material” as a low-cost and sustainable approach to recycle LIBs in the last 5 years. For instance, FVW derivatives such as tea and plant wastes,^{15,28} ethanol,²⁹ grape seed,³⁰ and macadamia shells³¹ were demonstrated to be effective organic reductants to enhance acid leaching of metals from spent LIBs. However, the compositional make-up of untreated FVW is a lot more complex compared to the existing inorganic reductants, which may potentially interfere with the post-leaching recovery of the metals and their downstream applications. Furthermore, to the best of our knowledge, functional applications of the metals extracted with the use of organic reductants have not been demonstrated. The search for greener alternative reducing agents remains a critical research gap in hydrometallurgy that has yet to be fully resolved.

To co-tackle the twin challenges of resource depletion and waste accumulation, a novel concept of using fruit peel waste as a possible reducing agent for the recycling of end-of-life LIB waste is proposed in this work. The purposeful exploitation of fruit-based waste products for the treatment of LIB waste is termed a “waste-for-waste” approach. Specifically, using pulverized orange peel (OP) as a prototypical fruit peel waste, the efficacy and safety of OP as a green reductant for the acid leaching of valuable metals from LIB cathode materials were examined. Organic H_3Cit lixiviant was chosen because it is biodegradable and has been shown to be effective as a leaching agent under mildly acidic pH.¹⁷ The reductive potential of OP was evaluated and it was shown that under optimized conditions, OP-mediated leaching efficiency of Co, Li, Mn, and Ni in LIB “black mass”-containing lixiviant is comparable to the use of H_2O_2 as the reducing agent. Furthermore, the selective recovery of $\text{Co}(\text{OH})_2$ can be achieved using the OP-inspired leaching system, which can subsequently be used to regenerate new batches of LCO coin cells.

■ EXPERIMENTAL SECTION

Materials and Reagents. Citric acid monohydrate, hydrochloric acid fuming 37%, sodium hydroxide pellets, 3,5-dinitrosalicylic acid, anhydrous glucose, and Soxhlet extraction apparatus were purchased from Sigma-Aldrich. Concentrated nitric acid (69%) and WHAT extraction thimble (43 × 123 mm) were purchased from VWR. Concentrated sulfuric acid (95–97%) and hydrogen peroxide (30% in H_2O) were purchased from Honeywell. ABTS assay kit was purchased from Beyotime, China. Dulbecco’s modified Eagle’s medium (DMEM, high glucose), fetal bovine serum (heat-inactivated), and antibiotic-antimycotic were purchased from GE HyClone. Resazurin sodium salt (AlamarBlue) was purchased from Sigma-Aldrich. All chemicals purchased and employed in this study were of analytical grade and solutions were prepared using Milli-Q ultrapure water.

The waste cathode material LCO and spent LIBs were kindly supplied by the School of Mechanical and Aerospace Engineering and School of Material Science and Engineering, Nanyang Technological University. SEM images of the LCO and spent LIBs are shown in Figure S1. The metallic composition of black mass was analyzed using inductively coupled plasma atomic emission spectroscopy (ICP-OES).

Preprocessing of Spent LIBs. The spent LCO cylindrical cells have a voltage that ranges from 3.1 to 3.4 V. To prevent flame and explosion hazards, the LCO batteries were fully discharged by submerging them in NaCl solution (20 wt %) overnight. The complete discharge of the batteries was confirmed using a battery tester (BT3554). Next, the fully discharged LCO batteries were shredded without prior dismantling using a custom-made shredder designed for battery processing (up to 10 kg/h) under inert gas conditions at room temperature. The shredded materials were then kept under exhaust suction overnight prior to being air-dried in a fume cupboard. Finally, the shredded materials were ground using a commercial food processor (JDC 3 L, 300 W) for approximately 1 min and sieved using a 60 μm mesh to remove the plastic constituents. The resultant fine particulate is termed black mass and was stored in a desiccator for subsequent experimentations.

Preparation and Characterization of OP. The OP was obtained from fresh oranges bought from a local supermarket.

The OP was immediately separated from the flesh and cut into pieces (~2 to 3 cm in length and ~2 to 4 mm in thickness). The samples were then oven-dried for 3 days at a constant temperature of 60 °C to ensure complete removal of moisture content. The dried OP was then pulverized and sieved with a #60 mesh (pore size, 250 μm). The composition, elemental analysis, and lignocellulosic constituent of OP employed in this study were characterized via established methodologies, as shown in Table S1.

The moisture content of OP was determined by comparing the weight difference before and after the oven drying process. The volatile content was obtained via thermogravimetric analysis (TGA) at a temperature increment rate of 50 °C per min and stabilized at 900 °C under a N₂ environment for 7 min. The ash content was acquired through TGA analysis at a temperature increment rate of 3 °C per min until it reached 700 °C under an O₂ environment. The fixed carbon content was calculated using the following expression

$$\text{fixed carbon\%} = 100\% - \text{moisture\%} - \text{volatile\%} - \text{ash\%} \quad (1)$$

The absolute elemental content was determined using the CHNS elemental analyzer. The oxygen content was calculated using the following expression³²

$$\text{oxygen\%} = 100\% - \text{C\%} - \text{H\%} - \text{N\%} - \text{S\%} - \text{ash\%} \quad (2)$$

The lignocellulosic composition of OP was quantified with the established protocols described elsewhere.³³ The cellulose content was calculated using the following expression

$$\text{cellulose\%} = 100\% - \text{extractive\%} - \text{hemicellulose\%} - \text{lignin\%} - \text{ash\%} \quad (3)$$

Reducing Sugar Measurements. The amount of reducing sugar in the OP samples was determined using the 3,5-dinitrosalicylic acid (DNS) method. To prepare the stock assay solution, DNS (1 g) was added to 2 mL of NaOH (2 M). The assay solution was then mixed with the OP sample solution (2:1, v/v) and boiled for 5 min. Reducing sugar-mediated conversion of the DNS into 3-amino-5-nitrosalicylic acid can be determined spectroscopically at a maximum absorbance wavelength of 540 nm (Molecular Devices SpectraMax M2). The equivalent concentration of reducing sugars (equiv to g/L glucose) of the OP samples was determined using glucose solutions with predetermined concentrations as standards.

Antioxidant Capacity Measurements. The antioxidant capacity (AC) of OP was determined using the ABTS assay kit (Beyotime). Prior to the measurement, a mixture of ABTS and oxidizer stock solution (1:1, v/v) was allowed to age in the dark at room temperature overnight. Next, the assay solution was prepared by diluting the mixture with PBS buffer with a dilution factor of 50. Trolox solutions of various concentrations (up to 0.2 mM) were prepared as per the manufacturer's protocol for normalization purpose. Readings were made on a 96-well format (Nunc, Thermo Fisher). Each well contains 10 μL of sample or trolox solution and 200 μL of assay solution reconstituted in 1 M H₃Cit. After 10 min of vigorous shaking, the absorbance was measured with a high-throughput microplate reader (Molecular Devices SpectraMax M2) at a maximum absorbance wavelength of 734 nm. AC was

computed and presented as "antioxidant capacity (equiv to mM trolox)".

Reductive Leaching. Leaching performance of OP in either LCO or black mass was examined in H₂Cit lixiviant. All the leaching experiments were conducted in a 100 mL round-bottom flask under reflux (water as a cooling agent) and stirring (350 rpm) conditions. The volume of the leaching solution (40 mL) was applied to all the experimental groups. Upon completion of the leaching experiments, the samples were allowed to cool down for 20 min before they were drawn out and transferred into 50 mL centrifuge tubes. Next, the residues were removed completely by ultracentrifugation at 8500 rpm for 10 min and the lixiviant was additionally passed through a 450 nm polyvinylidene fluoride (PVDF) membrane filter to remove any solid residues. The filtered lixiviant samples were kept at 4 °C for further use. To determine the ionic concentration of various metals in the lixiviant (1:500 dilution in deionized (DI) water), inductively coupled plasma atomic emission spectroscopy (ICP-OES) was used. Aqua regia was used for normalization purpose.³⁴ The leaching efficiency of each type of metal in the lixiviant can be calculated using the following expression

$$\text{leaching efficiency\%}(\text{Co, Li, Mn, Ni}) = \frac{\text{conc. (Co, Li, Mn, Ni) in a sample}}{\text{conc. (Co, Li, Mn, Ni) in aqua regia}} \times 100 \quad (4)$$

Cell Viability Assay. The toxic potential of the solid by-products (leaching residues) was examined using the alamarBlue cell viability assay in accordance to the manufacturer's recommended protocol. Briefly, solid residues after the leaching step was recovered, oven-dried (80 °C), and resuspended in water at 3 mg/mL (stock solution) by ultrasonication. To ensure sterility, the solution was under UV light (0.9 W) for 2 h prior to use. The panels of cell types used are (i) immortalized human keratinocytes (HaCaT), (ii) primary human dermal fibroblasts (HDF), and (iii) normal human colon mucosal epithelial cells (NCM460). Cells were seeded overnight to reach 70% confluency before the samples were treated with the leaching residues at various concentrations (i.e., 20, 50, 80, 100, 200, 500, and 1000 μg/mL) for 24 h. Cell viability was determined spectroscopically with fluorescence readout at an excitation/emission wavelength of 530/590 nm (Molecular Devices SpectraMax M2), as described earlier.^{35,36}

In Situ Precipitation of Metal Hydroxides. To prepare the leaching solution, 5 g of black mass and 1 g of OP were mixed with 100 mL of 1.5 M H₃Cit and allowed to react for 4 h at 100 °C. Following this, the leaching solution was centrifuged at 8500 rpm for 10 min. To remove the solid residues, the supernatant was then filtered using a 0.22 μm filter membrane (Nalgene, Thermo Scientific). NaOH was used to recover Co from the black mass leachate by forming cobalt (II/III) hydroxide ($K_{sp} = 5.92 \times 10^{-15}$ and 1.6×10^{-44} , respectively). To obtain cobalt hydroxide (II/III), the pH of the black mass leachate was first adjusted to 12 by addition of NaOH pellets to enable rapid precipitation of a hydroxide mixture that includes manganese hydroxide ($K_{sp} = 2 \times 10^{-13}$) and nickel hydroxide ($K_{sp} = 5.48 \times 10^{-16}$) along with a portion of cobalt hydroxide. Upon completion of the pH adjustment, the solution was immediately placed in the oven at the temperature of 80 °C for 30 min. The resultant cobalt-containing supernatant was then subjected to another round of

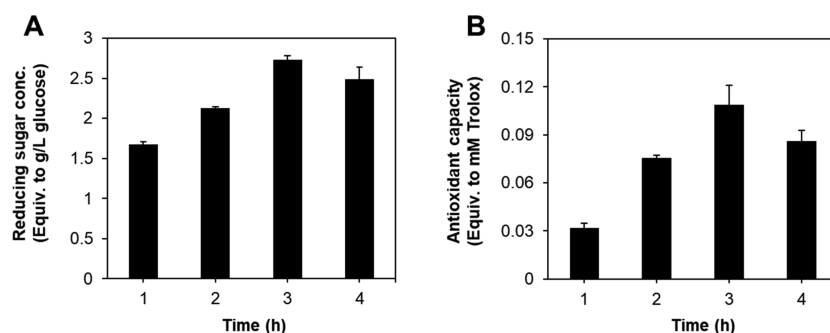


Figure 1. Time-course measurement of (A) reducing sugars and (B) antioxidant capacity of OP in H₃Cit (1 M). Reaction conditions: OP amount, 200 g; temperature, 90 °C.

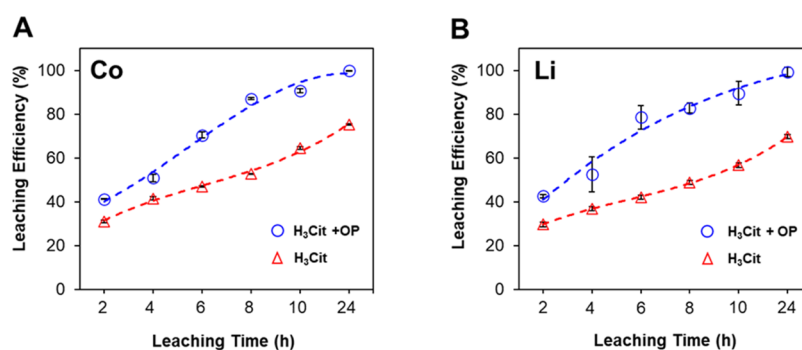


Figure 2. Time-dependent leaching efficiency of (A) Co and (B) Li in LCO solution using either H₃Cit (red open up-pointing triangle)- or H₃Cit + OP (blue open circle)-containing lixiviants. Leaching conditions: 40 mL of H₃Cit (1 M); OP, 200 mg; LCO = 500 mg; reaction temperature, 90 °C. Data are presented as mean \pm standard deviation.

precipitation via addition of ethanol (100%, $v_{\text{ethanol}}/v_{\text{supernatant}} = 1:10$) at the temperature of 80 °C overnight. The precipitate was retrieved by centrifugation, washed amply with water and oven-dried at 60 °C. Energy-dispersive X-ray spectroscopy (EDX) analysis revealed that the predominant oxide recovered using the OP approach is Co (II) hydroxide (Figure S2).

Regeneration of LCO Battery. To synthesize LCO, the recovered cobalt hydroxide was mixed with Li₂CO₃ (atomic ratio of Co/Li, 1:1.1). Excess Li was added to compensate for the thermal decomposition of Li during the thermal treatment.³⁷ The mixture was then calcined at 850 °C for 5 h to form LCO. The product after calcination was examined via X-ray diffraction (XRD) to determine its crystal structure.

Electrode slurry was prepared by mixing the recovered LCO, super P carbon, and PVDF binder (weight percent ratio, 80:10:10) in *N*-methyl-2-pyrrolidone (NMP) solvent. The slurry was coated onto an aluminum current collector and dried in the vacuum oven overnight at 90 °C. Li-ion coin cell batteries were fabricated in an Ar-filled glove box (MBRAUN) using this cathode and Li metal as the anode and LiPF₆ in ethylene carbonate (EC)/diethyl carbonate (DEC) as the electrolyte.

To assess the cyclic performance of the recycled Li-ion coin cell batteries, the batteries were subjected to galvanostatic charge–discharge testing at 0.1 C at a constant rate at room temperature using a Neware battery tester. The upper limit of the voltage used in the test was set to 5 V and the current was set to range from –1 to 1 mA. Voltage and current data were recorded every 30 s.

Statistical Analysis. All experiments in this study were triplicated. Data are presented by mean \pm standard deviation (SD). Origin 9 (OriginLab) was used for statistical analysis.

Experimental data were subjected to either Student's *t*-test or one-way analysis of variance (ANOVA) where applicable. Statistical differences are indicated with the probability value (*p* value) in the associated text or figure caption.

RESULTS AND DISCUSSION

Reductive Potential of OP Waste. It was postulated that the reducing capacity of OP could be attributed to two possible mechanisms of action. The first implicates the “reducing sugar theory”, as has been reported in several biomass-mediated leaching processes.^{38,39} When heated under acidic conditions, about 30% of the cellulose could be degraded into glucose and over 70% of the hemicellulose could be rapidly converted into aldehyde-containing reducing sugars as xylose, arabinose, and mannose.^{40–42} Oxidation of glucose can produce polyhydroxyacids, formic, gluconic, aldonic, and aldaric acids, aldoses, and CO₂.^{43,44} Figure 1A depicts the time-dependent production of reducing sugar by the OP samples at 90 °C in H₃Cit (1 M). As early as 1 h into the reaction, ~1.6 g/L equivalent concentration of glucose was detected in the reaction mix. The amount of reducing sugar continued to increase with reaction time and plateaued at 3 h with ~2.7 g/L equivalent concentration of glucose. Second, in addition to its cellulose-rich composition, another possible source of reducing components could stem from the presence of antioxidants such as phenolic acid and flavonoids, which could be hydrolyzed into reducing substances.⁴⁵ As shown in Figure 1B, a steady increase in the antioxidant capacity (AC) of OP was observed from 1 h onward and the maximal AC of 0.108 equiv to mM trolox was obtained at around 3 h. The slight decrease in the AC of the OP at 4 h may be explained by the thermal instability of antioxidants, which could undergo

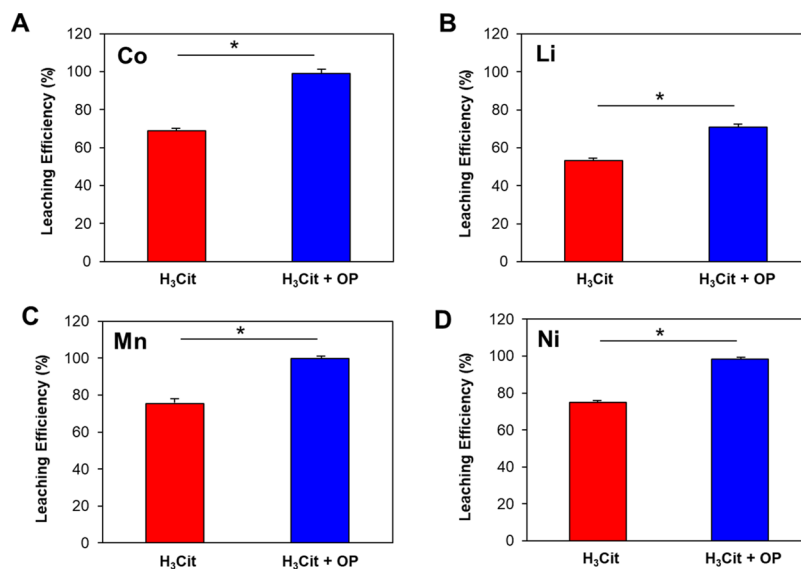


Figure 3. Leaching efficiency of (A) Co, (B) Li, (C) Mn, and (D) Ni in LIB black mass-containing lixiviant using either H₃Cit or H₃Cit + OP. Leaching conditions: H₃Cit (1 M); lixiviant volume, 40 mL; OP, 200 mg; LCO, 500 mg; black mass, 200 mg; leaching temperature, 90 °C; leaching duration, 7 h. Data are presented as mean \pm standard deviation. Asterisk (*) denotes the significant difference between the indicated experimental groups. $p < 0.05$.

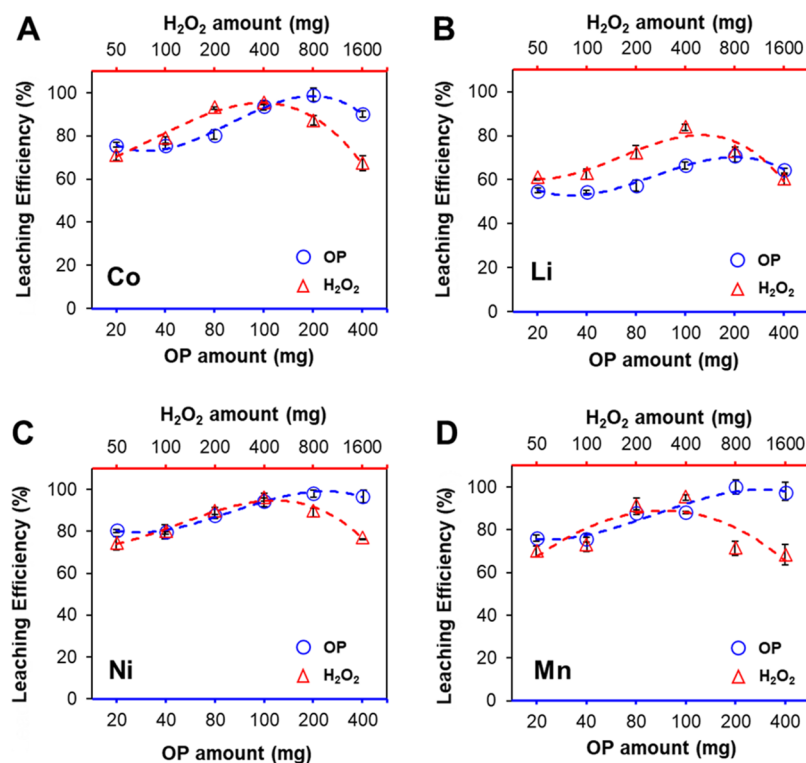


Figure 4. Effect of reductant amount on the leaching efficiency of (A) Co, (B) Li, (C) Ni, and (D) Mn in LIB black mass-containing lixiviant using either OP (blue open circle) or H₂O₂ (red open up-pointing triangle) as the reductant. Leaching conditions: H₃Cit (1 M); lixiviant volume, 40 mL; black mass, 200 mg; leaching temperature, 90 °C; leaching duration, 4 h. Data are presented as mean \pm standard deviation.

structural decomposition when heated at 100 °C.⁴⁶ Therefore, these findings suggest that OP is a promising H₂O₂ substitute for hydrometallurgical processes as it contains numerous reducing constituents.

OP Waste as a Leaching Agent. Having established the reducing properties of OP, the performance of OP as a leaching agent using LCO solution in H₃Cit lixiviant was next evaluated. The experimental group without the addition of OP

serves as a control. As shown in Figure 2A, without the addition of OP, the leaching efficiency of Li and Co from LCO increased with time but only managed to peak at 70% and 75%, respectively, 24 h into the experiment. In contrast, the leaching efficiencies of Li and Co in the OP-containing lixiviant were clearly enhanced at each time step relative to the H₃Cit-only group. Maximal increment in leaching efficiency of ~35% for Li and Co for the OP + H₃Cit group occurs at the 6 and 8 h

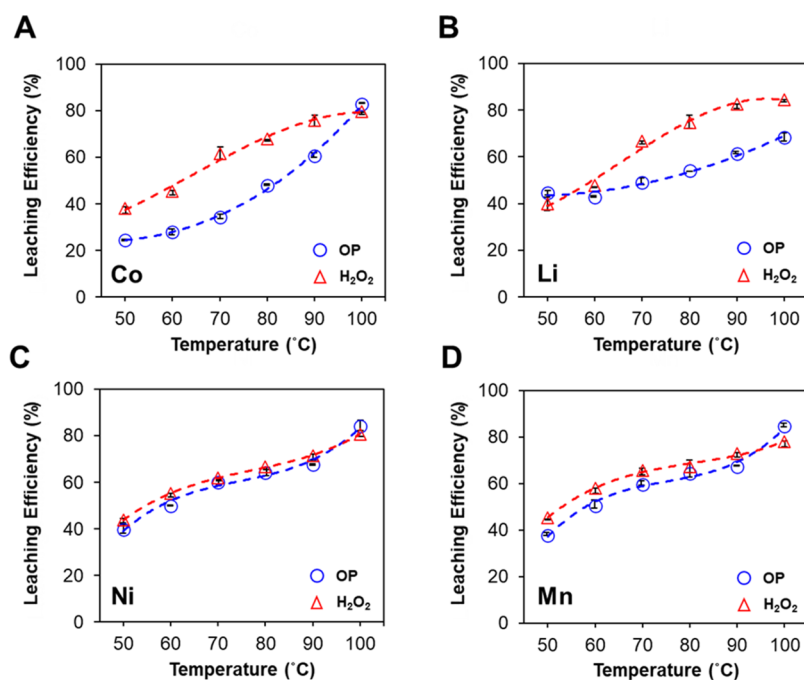


Figure 5. Effect of temperature on the leaching efficiency of (A) Co, (B) Li, (C) Ni, and (D) Mn in LIB black mass-containing lixiviant using either OP (blue open circle) or H₂O₂ (red open up-pointing triangle) as the reductant. Leaching conditions: H₃Cit (1 M); lixiviant volume, 40 mL; OP, 200 mg; H₂O₂, 400 mg; black mass, 200 mg; leaching duration, 4 h. Data are presented as mean \pm standard deviation.

marks, respectively. By 24 h, complete (100%) leaching of both metallic ions was observed in the OP + H₃Cit group.

Having established the leaching properties of OP in pure LCO samples, the leaching performance of OP using actual spent LIB waste (i.e., black mass) was next examined. In terms of chemical composition, black mass is far more complex compared to the LCO sample. ICP-OES analysis of the elemental composition of the black mass revealed that apart from Li (4.7%) and Co (35.5%), other metallic constituents such as Mn (2.1%), Ni (3.1%), Al (1.7%), and Cu (1.4%) were also found to be present in the complex waste materials (data not shown). The Al and Cu ions are most likely to originate from the current collectors. Figure 3 shows the leaching efficiencies of the main cathode materials (i.e., Co, Li, Mn, and Ni) in the LIB black mass sample. In the H₃Cit-only group, the leaching efficiencies of the various metals vary and are limited to <80% regardless of the identity of the metal. Conversely, the addition of OP to the lixiviant resulted in a substantial increase in the amount of extracted metals by ~17–30%. Except for Li, which has a leaching efficiency of ~70%, a near 100% recovery of Co, Ni, and Mn could be achieved from the OP- and H₃Cit-containing lixiviants. Taken together, these results show that pulverized OP waste can indeed be exploited to recover cathode metals from not only the pristine LCO sample but also actual spent LIB waste.

Optimization of OP-Mediated Leaching Conditions.

The effects of several parameters were systematically examined and correlated to the leaching efficiency of the different metals in the black mass-containing lixiviant.

Effect of Reductant Amount. The effect of varying the amount of OP reductant on the leaching experiments was first examined. H₂O₂, a widely used reductant in the metal extraction process, was employed as a basis of comparison. The amount of OP and H₂O₂ was varied from 20–400 mg to 50–1600 mg per batch of reaction. In general, the leaching

efficiency increased with increasing amount of OP and H₂O₂ (Figure 4). For the H₂O₂ group, optimal dissolution of the metals was observed with 400 mg (1%, v/v) of reductant, which is in agreement with an earlier study that involved the leaching of Co, Li, Ni, Cu, Mn, and Al from LIB waste in HCl (4 M).⁴⁷ As shown in Figure 4, more than 90% of Co, Mn, and Ni and ~80% of Li could be recovered at this concentration. However, at higher amount of H₂O₂, a drastic decrease was observed in the leaching efficiencies for all the metals by as much as 20%. This could be attributed to the concentration-dependent self-decomposition of H₂O₂, which will severely decrease the availability of the reductant (i.e., H₂O₂) in the leaching solution.¹⁴ In the case of the OP group, maximal Co (98.9%), Li (72.5%), Ni (98.2%), and Mn (99.8%) and recovery were observed with 200 mg of OP powder. However, in contrast to the H₂O₂ group, metal leaching efficiencies did not decrease but plateaued at a near-maximum, with increasing OP concentration. It should be highlighted that in terms of the leaching efficiency, the potency of both reductants is on par, even if the mass of H₂O₂ are at several-fold higher than the mass of OP used.

Effect of Leaching Temperature. Having established the optimal amount of reductant (i.e., 200 mg of OP and 400 mg of H₂O₂) from the previous section, the effect of temperature on the leaching process was next examined. Temperature has important bearing on the thermodynamics and kinetics of the metal leaching.⁴⁸ Shown in Figure 5 are the leaching efficiencies of both reductants for Co, Li, Mn, and Ni over a reaction temperature range of 50–100 °C and a reaction time of 4 h. Increasing the leaching temperature led to a progressive and considerable increase in the leaching efficiency for all the metallic ions regardless of reductant type. Similar temperature-dependent trend was also reported by Natarajan et al. with H₂O₂ used as the reductant.⁴⁹ When the leaching temperature was increased from 50 to 100 °C, corresponding increases of

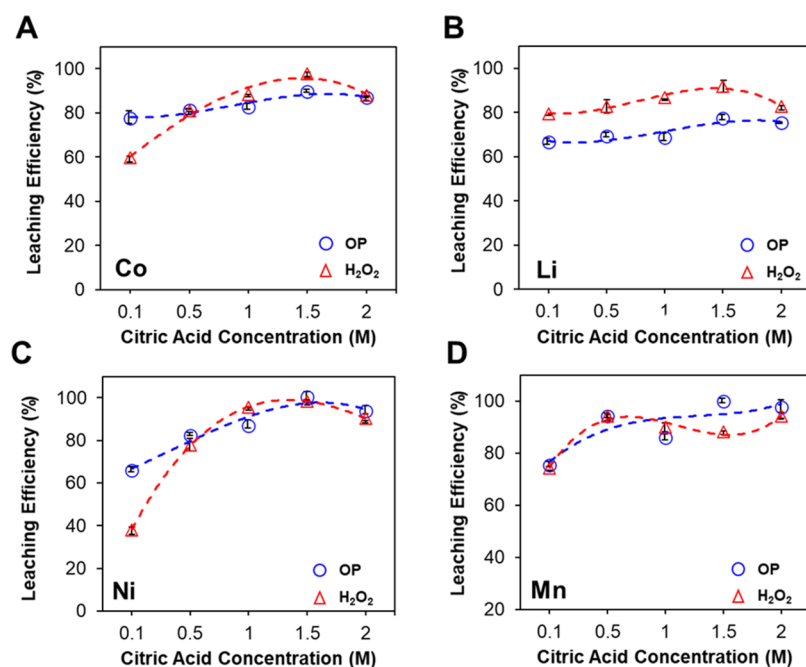


Figure 6. Effect of H₃Cit concentration on the leaching efficiency of (A) Co, (B) Li, (C) Ni, and (D) Mn in LIB black mass-containing lixiviant using either OP (blue open circle) or H₂O₂ (red open up-pointing triangle) as the reductant. Leaching conditions: lixiviant volume, 40 mL; OP, 200 mg; H₂O₂, 400 mg; black mass, 200 mg; leaching temperature, 100 °C; leaching duration, 4 h. Data are presented as mean \pm standard deviation.

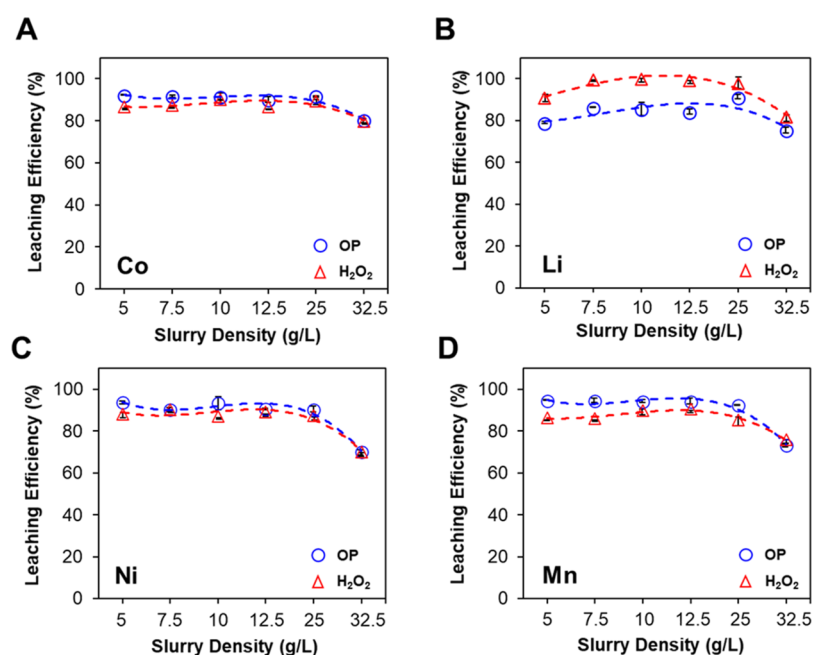


Figure 7. Effect of slurry density ($w_{\text{black mass}}/v_{\text{lixiviant solution}}$) on the leaching efficiency of (A) Co, (B) Li, (C) Ni, and (D) Mn in LIB black mass-containing lixiviant using either OP (blue open circle) or H₂O₂ (red open up-pointing triangle) as the reductant. Leaching conditions: H₃Cit (1.5 M); lixiviant volume, 40 mL; OP, 200 mg; H₂O₂, 400 mg; leaching temperature, 100 °C; leaching duration, 4 h. Data are presented as mean \pm standard deviation.

55%, 25%, 41%, and 47% for Co, Li, Ni, and Mn were observed, respectively. Specifically, at the leaching temperature of 100 °C, 82% of Co, 68% of Li, 84% of Ni, and 84% of Mn were found to be leached into the lixiviant. Therefore, with the other parameters kept constant, it can be concluded that 100 °C would be the ideal temperature to maximize the leaching capacity of OP.

Effect of Acid Concentration. Earlier studies have shown that acid concentration is a critical determinant of the leaching process.^{15,50} In the proposed leaching systems, an acidic milieu can potentially favor the redox reaction to generate different forms of metallic ions, as shown in formula 5. Additionally, increasing the ionic strength of the lixiviant is also postulated to promote the decomposition of cellulose and hemicellulose

found in the OP into reducing sugars, thereby aiding the leaching process.⁵¹

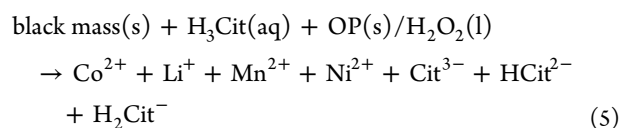
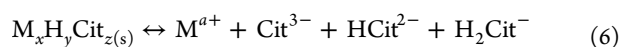


Figure 6 shows the plot of leaching efficiency with increasing concentration of H₃Cit from 0.1 to 2.0 M. The highest amount of extracted Co (89%), Li (76%), Ni (100%), and Mn (100%) occurs when 1.5 M H₃Cit was used with OP as the reductant. This is consistent with an earlier study by Chen et al., in which maximal leaching of Co was attained with the same concentration of H₃Cit in 1% H₂O₂.¹⁵ Interestingly, dissolved fraction of Co and Li only improved by ~10% when H₃Cit was increased from 0.2 to 1.5 M. Comparatively, higher concentration of H₃Cit leads to about 25–35% enhancement in Ni and Mn leaching. However, the leaching efficiency of these metals began to plateau off or decline slightly in both the OP- and H₂O₂-based leaching systems when the concentration of H₃Cit was increased from 1.5 to 2.0 M. A possible explanation could be attributed to formation of insoluble metallic citrates (e.g., Co₃Cit₂) when H₃Cit is added in excess (see formula 6). Therefore, increasing the H₃Cit concentration to a certain extent is likely to result in the observed level-off/decline in leaching efficiency by the salting-out effects.⁵²



where M denotes Mn/Ni/Co/Li; subscripts *x*, *y*, and *z* denote the number of element in the molecule; and superscript *a* denotes the valency of the different metals.

Effect of Slurry Density. Slurry density was varied by controlling the black mass-to-leaching liquid ratio. The slurry density has a marginal effect on the leaching efficiency in both the OP and H₂O₂ groups up to a concentration of 25 g/L (Figure 7). Despite the relative high slurry density, the leaching efficiency in the OP group was >90%. However, when the slurry density was further increased from 25 to 32.5 g/L, there was a significant decrease (~15%) in the leaching efficiency for all the metallic ions probed. These findings were corroborated by a number of earlier works, which similarly showed that slurry densities ranging from 15 to 30 g/L were favorable for leaching of cathode materials.^{15,49,53} In addition, the results also suggest that beyond the slurry density of 25 g/L, the amount of H₃Cit and OP may be limiting.

Taken together, these findings revealed that the combination of various parameters (200 mg of OP, leaching temperature of 100 °C, H₃Cit (1.5 M), leaching duration of 4 h, and slurry density of 25 g/L) could significantly augment the leaching efficiency of the OP-enabled hydrometallurgy. With this set of conditions, Co (91.3%), Li (80.5%), Ni (90.1%), and Mn (92.2%) were recovered from the black mass lixiviant. This set of conditions can serve as a baseline condition for future scale-up and optimization.

Characterization and Toxicity Evaluation of By-Products Derived from the Leaching Process. The sustainable utilization of OP-enabled hydrometallurgy would also require that the generated side-streams be environmentally friendly and safe. The elemental composition of the residual materials was first determined using energy-dispersive X-ray spectroscopy (EDX). As can be seen in Figure 8A, the solid by-products contain largely C (64.2%), O (33.3%), and trace

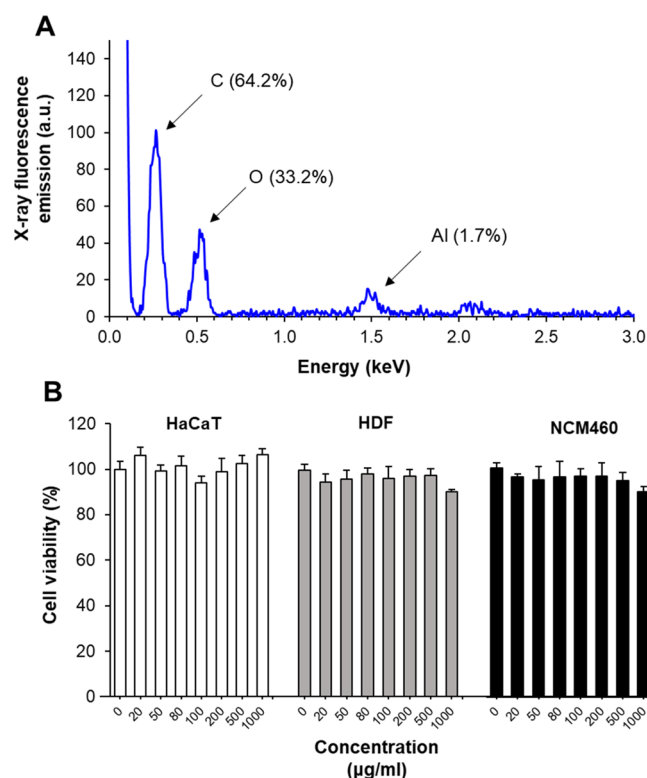


Figure 8. (A) X-ray fluorescence spectrum of the solid residue by-product. Relative (%) abundance of the detected elements are indicated in the parentheses. (B) Cell viability of HaCaT, HDF, and NCM460 exposed to the solid residues at concentrations ranging from 0 to 1000 µg/mL. Data are presented as mean ± SD derived from three independent experiments.

amount of Al (1.6%), suggesting that the residue is likely to originate from the anode (graphite) and OP waste (organic compounds). Since the impact of these materials on human health is one key reflection of their environmental footprints, the toxic potential of the solid residues was evaluated using the alamarBlue assay in three different human cell lines, namely, (i) human keratinocytes (HaCaTs), (ii) human colorectal cells (NCM460), and (iii) human dermal fibroblasts (HDF). Figure 8B shows the dose–response graph of the respective cells that were exposed to the leachate solid waste with a concentration ranging from 0 to 1000 µg/mL. Remarkably, the cytotoxic potential of the by-products was negligible in all tested cell lines, even at the extreme concentration of 1000 µg/mL. This suggests that the carbonaceous by-product is nontoxic and by extension, its environmental impact should be minimal. Nevertheless, to better evaluate the long-term environmental impact of the OP leaching-derived carbonaceous by-product, other chemical analysis such as toxicity characteristic leaching procedure (TCLP) can be employed to simulate the leaching process in the landfill setting.⁵⁴

Recovery of Co and Regeneration of New Lithium-Ion Batteries. To assess the applicability of the OP-enabled hydrometallurgy to the LIB recycling industry, Co was retrieved from the OP leaching liquor with the aim to be subsequently used to generate new batches of LCO batteries. A two-step NaOH-induced precipitation protocol was employed to retrieve cobaltous hydroxide. In the first step, the pH of the leachate was adjusted to 12 using NaOH to induce rapid precipitation and removal of Mn(OH)₂ and Ni(OH)₂. At this

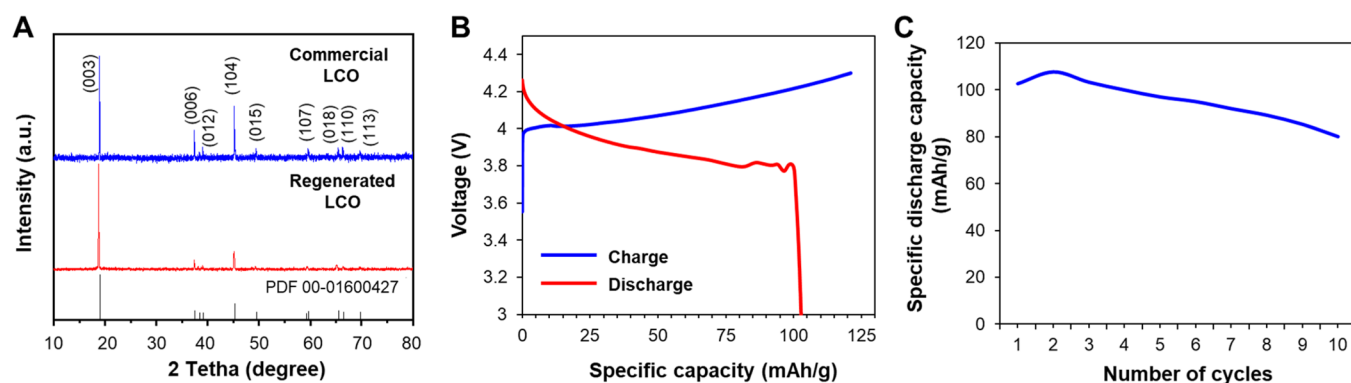


Figure 9. (A) XRD pattern of the commercial (blue) and regenerated (red) LCO. (B) Initial charge (blue)–discharge (red) performance of the regenerated LCO coin cell and (C) stability of discharge capacity over 10 cycles of charge and discharge.

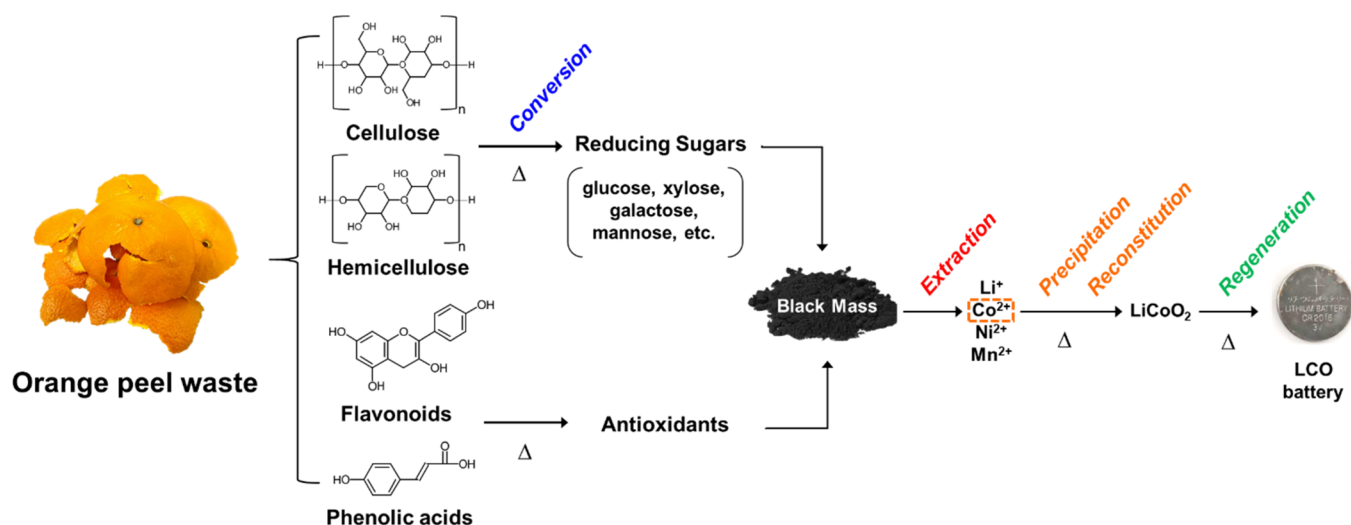


Figure 10. Mechanistic and process summary of OP-enabled recycling of spent LIBs.

pH, the precipitation of $\text{Cu}(\text{OH})_2$ and $\text{Al}(\text{OH})_3$ is largely prohibited due to the amphoteric nature of the two hydroxides, which makes them soluble in highly alkaline conditions. Thereafter, in the second step, the Co-rich lixiviant was subjected to another round of precipitation using ethanol (100%, $v_{\text{ethanol}}/v_{\text{supernatant}} = 1:10$) to recover cobalt hydroxide. The chemical characteristics of the recovered precipitate were further examined using EDX (Figure S2). On the basis of the atomic weight ratio of Co and O, it strongly suggests that the retrieved precipitate is $\text{Co}(\text{OH})_2$ with traces of Al (6.76%) and Cu (1.42%) impurities. Additionally, recovery efficiency of Co across four independent batches of OP leachate displayed good consistency with an average recovery rate of >73% (Figure S3).

To prepare LCO, the dried precipitate of $\text{Co}(\text{OH})_2$ was mixed with lithium carbonate (atomic ratio, 1:1.1) and subjected to thermal treatment at 850 °C for 5 h. Successful formation of single-phase LCO (rhombohedral $R\bar{3}m$ space group crystal system) was validated by examining the crystal structure of the calcined product via X-ray powder diffraction (XRD). The XRD diffraction pattern of the calcined materials exhibited a good match with the commercial LCO (Figure 9A). Coin cell batteries were assembled using the recycled LCO as the cathode material. Battery performance was evaluated using the galvanostatic charge–discharge test. Cyclic performance data revealed that the newly generated LIBs from the black mass samples possessed a comparable initial charge

capacity to the commercial LIBs (~ 120 mAh/g) and the initial discharge capacity was approximately 103 mAh/g (Figure 9B). Further analysis revealed that the recycled LIBs had a desirable stable performance within 10 cycles of charge and discharge, with less than 20% capacity loss in the 10th cycle (Figure 9C). This suggests that this new technology is practically feasible for recycling spent LIBs in the industrial sense.

In summary, the novel use of pulverized OP as an organic, low-cost, and effective green reductant for the recovery of cathodic metals from spent LIBs was demonstrated (Figure 10). The reductive potential of OP can be attributed to the thermal conversion of cellulose to reducing sugars as well as the presence of naturally occurring antioxidants such as flavonoids and phenolic acids. Addition of OP notably enhanced the leaching performance of H_3Cit lixiviant to obtain a 100% extraction yield of Co and Li from pure LCO samples. Both H_2O_2 and OP reductants showed comparable recovery efficacy of Co, Li, Ni, and Mn or around 90% in LIB black mass-containing leaching liquor, even at a relatively high slurry density of 25 g/mL. Further studies are warranted to improve the leaching efficiency of the OP approach. Among the possible strategies may include the optimization of stirring speed and leaching time to increase the homogeneity of the leaching suspension, as well as the adoption of a continuous flow setup to precisely control the flow rate of the feed reactants. Importantly, solid residues generated from the OP-

enabled hydrometallurgy process were found to be nontoxic, suggesting that the approach is environmentally sound. Although not covered in this work, clarifying the reusability of the generated OP solid waste for the follow-up leaching process would be of interest since this can potentially further lower the operational cost. Finally, to “close the waste loop”, a two-step precipitation process was employed to selectively retrieve $\text{Co}(\text{OH})_2$ from the leachate to prepare single-phase LCO, from which new batches of functional LCO coin cell batteries were regenerated. However, the performance characteristics of the recycled battery can be further improved as the presence of Cu and Al may have affected the overall rate performance of the battery. Targeted removal of Cu and Al may be facilitated by pH adjustment to control the solubility of the metal hydroxides^{55,56} or use of carboxylate or bipyridine ligands.⁵⁷ Furthermore, this “waste-for-waste” approach could also potentially be extended to other types of cellulose-rich FVW, as well as lithium-ion battery types (e.g., lithium manganese oxide (LMO), lithium nickel manganese cobalt oxide (LNMCO), etc.) for the new circular economy of E-waste so that our lives can be powered in a greener and more sustainable manner.

■ ASSOCIATED CONTENT

SI Supporting Information

The Supporting Information is available free of charge at <https://pubs.acs.org/doi/10.1021/acs.est.0c02873>.

Compositional analysis of orange peel (OP) (Table S1), SEM images of pure LCO and LIB black mass (Figure S1), X-ray fluorescence spectrum of the recovered cobalt hydroxide (Figure S2), and recovery efficiency of Co retrieved from four different batches of the OP leaching solution (Figure S3) (PDF)

■ AUTHOR INFORMATION

Corresponding Authors

Madhavi Srinivasan – Energy Research Institute and School of Materials Science and Engineering, Nanyang Technological University, 637553, Singapore; Email: madhavi@ntu.edu.sg

Chor Yong Tay – Energy Research Institute, School of Materials Science and Engineering, and School of Biological Sciences, Nanyang Technological University, 637553, Singapore;

ORCID.org/0000-0001-6721-7106; Email: cytay@ntu.edu.sg

Authors

Zhuoran Wu – Energy Research Institute, Nanyang Technological University, 637553, Singapore

Tanto Soh – Energy Research Institute, Nanyang Technological University, 637553, Singapore

Jun Jie Chan – Energy Research Institute and School of Materials Science and Engineering, Nanyang Technological University, 637553, Singapore

Shize Meng – School of Materials Science and Engineering, Nanyang Technological University, 639798, Singapore

Daniel Meyer – Institut de Chimie Séparative de Marcoule (ICSM), UMR 5257 CEA-CNRS-UM-ENSCM, 30207 Bagnols-sur-Cèze Cedex, France

Complete contact information is available at: <https://pubs.acs.org/doi/10.1021/acs.est.0c02873>

Author Contributions

The manuscript was written through contributions of all authors. All authors have given approval to the final version of the manuscript.

Funding

SCARCE is supported by the National Research Foundation, Prime Minister's Office, Singapore, the Ministry of National Development, Singapore, and National Environment Agency, Ministry of the Environment and Water Resource, Singapore under the Closing the Waste Loop R&D Initiative as part of the Urban Solutions & Sustainability–Integration Fund (award no. USS-IF-2018-4).

Notes

The authors declare no competing financial interest.

■ ABBREVIATIONS

AC	antioxidant capacity
ANOVA	one-way analysis of variance
H ₃ Cit	citric acid
DEC	diethyl carbonate
DNS	3,5-dinitrosalicylic acid solution
EC	ethylene carbonate
EDX	energy-dispersive X-ray spectroscopy
FVW	fruit and vegetable waste
HaCaT	immortalized human keratinocytes
HDF	primary human dermal fibroblasts
ICP-OES	inductively coupled plasma atomic emission spectroscopy
LIBs	lithium-ion batteries
NCM460	normal human colon mucosal epithelial cell
NMP	N-methyl-2-pyrrolidone
OP	orange peel
SD	standard deviation
TGA	thermogravimetric analysis
W-for-W	waste for waste
XRD	X-ray diffraction

■ REFERENCES

- (1) Li, J.; Zeng, X.; Chen, M.; Ogunseitan, O. A.; Stevels, A. “Control-alt-delete”: rebooting solutions for the E-waste problem. *Environ. Sci. Technol.* **2015**, *49*, 7095–7108.
- (2) Shi, Y.; Chen, G.; Chen, Z. Effective regeneration of LiCoO₂ from spent lithium-ion batteries: a direct approach towards high-performance active particles. *Green Chem.* **2018**, *20*, 851–862.
- (3) *Lithium-ion Battery - Global Market Outlook (2017-2026)*, www.strategyfirst.com/report/lithium-ion-battery-market%20 (2018).
- (4) Xiao, J.; Li, J.; Xu, Z. Challenges to Future Development of Spent Lithium Ion Batteries Recovery from Environmental and Technological Perspectives. *Environ. Sci. Technol.* **2020**, *54*, 9–25.
- (5) Barbaschow, A. CSIRO: Lithium-ion battery waste to exceed 100,000 tonnes by 2036. <https://www.zdnet.com/article/csiro-lithium-ion-battery-waste-to-exceed-100000-tonnes-by-2036/>, 2018.
- (6) Gardiner, J. The rise of electric cars could leave us with a big battery waste problem. <https://www.theguardian.com/sustainable-business/2017/aug/10/electric-cars-big-battery-waste-problem-lithium-recycling>, 2017.
- (7) Kang, D. H. P.; Chen, M.; Ogunseitan, O. A. Potential environmental and human health impacts of rechargeable lithium batteries in electronic waste. *Environ. Sci. Technol.* **2013**, *47*, 5495–5503.
- (8) Staff, S. The Role of Cobalt in the Lithium Battery Market. <https://www.fierceelectronics.com/components/role-cobalt-lithium-battery-market>.
- (9) Yun, L.; Linh, D.; Shui, L.; Peng, X.; Garg, A.; Le, M. L. P.; Asghari, S.; Sandoval, J. Metallurgical and mechanical methods for

recycling of lithium-ion battery pack for electric vehicles. *Resour., Conserv. Recycl.* **2018**, *136*, 198–208.

(10) Horeh, N. B.; Mousavi, S. M.; Shojaosadati, S. A. Bioleaching of valuable metals from spent lithium-ion mobile phone batteries using *Aspergillus niger*. *J. Power Sources* **2016**, *320*, 257–266.

(11) Setyawati, M. I.; Xie, J.; Leong, D. T. Phage based green chemistry for gold ion reduction and gold retrieval. *ACS Appl. Mater. Interfaces* **2014**, *6*, 910–917.

(12) Bosecker, K. Bioleaching: metal solubilization by micro-organisms. *FEMS Microbiol. Rev.* **1997**, *20*, 591–604.

(13) Huang, B.; Pan, Z.; Su, X.; An, L. Recycling of lithium-ion batteries: Recent advances and perspectives. *J. Power Sources* **2018**, *399*, 274–286.

(14) Fungene, T.; Groot, D. R.; Mahlangu, T.; Sole, K. C. Decomposition of hydrogen peroxide in alkaline cyanide solutions. *J. South. Afr. Inst. Min. Metall.* **2018**, *118*, 1259.

(15) Chen, X.; Luo, C.; Zhang, J.; Kong, J.; Zhou, T. Sustainable Recovery of Metals from Spent Lithium-Ion Batteries: A Green Process. *ACS Sustainable Chem. Eng.* **2015**, *3*, 3104–3113.

(16) Li, L.; Dunn, J. B.; Zhang, X. X.; Gaines, L.; Chen, R. J.; Wu, F.; Amine, K. Recovery of metals from spent lithium-ion batteries with organic acids as leaching reagents and environmental assessment. *J. Power Sources* **2013**, *233*, 180–189.

(17) Brisson, V. L.; Zhuang, W.-Q.; Alvarez-Cohen, L. Bioleaching of rare earth elements from monazite sand. *Biotechnol. Bioeng.* **2016**, *113*, 339–348.

(18) Gao, W.; Zhang, X.; Zheng, X.; Lin, X.; Cao, H.; Zhang, Y.; Sun, Z. Lithium Carbonate Recovery from Cathode Scrap of Spent Lithium-Ion Battery: A Closed-Loop Process. *Environ. Sci. Technol.* **2017**, *51*, 1662–1669.

(19) Li, L.; Ge, J.; Wu, F.; Chen, R.; Chen, S.; Wu, B. Recovery of cobalt and lithium from spent lithium ion batteries using organic citric acid as leachant. *J. Hazard. Mater.* **2010**, *176*, 288–293.

(20) Chen, X.; Kang, D.; Cao, L.; Li, J.; Zhou, T.; Ma, H. Separation and recovery of valuable metals from spent lithium ion batteries: Simultaneous recovery of Li and Co in a single step. *Sep. Purif. Technol.* **2019**, *210*, 690–697.

(21) Atkinson, D. A.; Sim, T. C.; Grant, J. A. Sodium metabisulfite and SO₂ release - an under-recognized hazard among shrimp fishermen. *Ann. Allergy* **1994**, *71*, 563.

(22) Meshram, P.; Abhilash; Pandey, B. D.; Mankhand, T. R.; Deveci, H. Comparison of Different Reductants in Leaching of Spent Lithium Ion Batteries. *Jom* **2016**, *68*, 2613–2623.

(23) Meshram, P.; Pandey, B. D.; Mankhand, T. R. Hydrometallurgical processing of spent lithium ion batteries (LIBs) in the presence of a reducing agent with emphasis on kinetics of leaching. *Chem. Eng. J.* **2015**, *281*, 418–427.

(24) Ong, K. L.; Kaur, G.; Pensupa, N.; Uisan, K.; Lin, C. S. K. Trends in food waste valorization for the production of chemicals, materials and fuels: Case study South and Southeast Asia. *Bioresour. Technol.* **2018**, *248*, 100–112.

(25) Vanham, D.; Bouraoui, F.; Leip, A.; Grizzetti, B.; Bidoglio, G. Lost water and nitrogen resources due to EU consumer food waste. *Environ. Res. Lett.* **2015**, *10*, No. 084008.

(26) Zafar, S. *Food Waste Management in USA*. <https://www.bioenergyconsult.com/trends-in-food-waste-management/>, 2019.

(27) Kumar, K.; Yadav, A. N.; Kumar, V.; Vyas, P.; Dhaliwal, H. S. Food waste: a potential bioresource for extraction of nutraceuticals and bioactive compounds. *Bioresour. Bioprocess.* **2017**, *4*, 18.

(28) Chen, Y.; Chang, D.; Liu, N.; Hu, F.; Peng, C.; Zhou, X.; He, J.; Jie, Y.; Wang, H.; Wilson, B. P.; Lundstrom, M. Biomass-Assisted Reductive Leaching in H₂SO₄ Medium for the Recovery of Valuable Metals from Spent Mixed-Type Lithium-Ion Batteries. *Jom* **2019**, *71*, 4465–4472.

(29) Zhao, J.; Zhang, B.; Xie, H.; Qu, J.; Qu, X.; Xing, P.; Yin, H. Hydrometallurgical recovery of spent cobalt-based lithium-ion battery cathodes using ethanol as the reducing agent. *Environ. Res.* **2020**, *181*, 108803.

(30) Zhang, Y.; Meng, Q.; Dong, P.; Duan, J.; Lin, Y. Use of grape seed as reductant for leaching of cobalt from spent lithium-ion batteries. *J. Ind. Eng. Chem.* **2018**, *66*, 86–93.

(31) Zhao, Y.; Liu, B.; Zhang, L.; Guo, S. Microwave Pyrolysis of Macadamia Shells for Efficiently Recycling Lithium from Spent Lithium-ion Batteries. *J. Hazard. Mater.* **2020**, *396*, 122740.

(32) Firdaus, A. R. M.; Samah, M. A. A.; Hamid, K. B. A. CHNS analysis towards food waste in composting. *J. CleanWAS* **2018**, *2*, 06.

(33) Ayeni, A. O.; Adeeyo, O. A.; Oresegun, O. M.; Oladimeji, T. E. Compositional analysis of lignocellulosic materials: Evaluation of an economically viable method suitable for woody and non-woody biomass. *Am. J. Eng. Res.* **2015**, *4*, 14.

(34) Jadhav, U.; Hocheng, H. Hydrometallurgical Recovery of Metals from Large Printed Circuit Board Pieces. *Sci. Rep.* **2015**, *5*, 14574.

(35) Wu, Z.; Yang, H.; Archana, G.; Rakshit, M.; Ng, K. W.; Tay, C. Y. Human keratinocytes adapt to ZnO nanoparticles induced toxicity via complex paracrine crosstalk and Nrf2-proteasomal signal transduction. *Nanotoxicology* **2018**, *12*, 1215–1229.

(36) Wu, Z.; Shi, P.; Lim, H. K.; Ma, Y.; Setyawati, M. I.; Bitounis, D.; Demokritou, P.; Ng, K. W.; Tay, C. Y. Inflammation Increases Susceptibility of Human Small Airway Epithelial Cells to Pneumonic Nanotoxicity. *Small* **2020**, 2000963.

(37) Antolini, E.; Ferretti, M. Synthesis and Thermal Stability of LiCoO₂. *J. Solid State Chem.* **1995**, *117*, 1–7.

(38) Hariprasada, D.; Dash, B.; Ghosh, M. K.; Anand, S. Leaching of manganese ores using sawdust as a reductant. *Miner. Eng.* **2007**, *20*, 1293–1295.

(39) Tian, X.; Wen, X.; Yang, C.; Liang, Y.; Pi, Z.; Wang, Y. Reductive leaching of manganese from low-grade manganese dioxide ores using corncob as reductant in sulfuric acid solution. *Hydrometallurgy* **2010**, *100*, 157–160.

(40) Pessoa, A., Jr.; Mancilha, I. M.; Sato, S. Acid Hydrolysis of Hemicellulose from Sugarcane Bagasse. *Braz. J. Chem. Eng.* **1997**, *14*, 00.

(41) Amirkhani, H.; Yunus, R.; Rashid, U.; Salleh, S. F.; Radhiah, A. B. D.; Syam, S. Low-Temperature Dilute Acid Hydrolysis of Oil Palm Frond. *Chem. Eng. Commun.* **2014**, *202*, 1235–1244.

(42) Bouchard, J.; Overend, R. P.; Chornet, E.; Van Calsteren, M.-R. Mechanism of Dilute Acid Hydrolysis of Cellulose Accounting for its Degradation in the Solid State. *J. Wood Chem. Technol.* **1992**, *12*, 335–354.

(43) Marcq, O.; Barbe, J.-M.; Trichet, A.; Guillard, R. Reaction pathways of glucose oxidation by ozone under acidic conditions. *Carbohydr. Res.* **2009**, *344*, 1303–1310.

(44) Zhu, H.; Li, L.; Zhou, W.; Shao, Z.; Chen, X. Advances in non-enzymatic glucose sensors based on metal oxides. *J. Mater. Chem. B* **2016**, *4*, 7333–7349.

(45) Mohan, A. C. Screening of Total Phenol, Cellulose and Tannin Content in Orange Peel by Using Different Parameters in Ethanol Extract. *World J. Pharma. Res.* **2017**, *10*, 1049–1058.

(46) Hamama, A. A.; Nawar, W. W. Thermal decomposition of some phenolic antioxidants. *J. Agric. Food Chem.* **1991**, *39*, 1063–1069.

(47) Aaltonen, M.; Peng, C.; Wilson, B.; Lundström, M. Leaching of Metals from Spent Lithium-Ion Batteries. *Recycling* **2017**, *2*, 20.

(48) Torres, R.; Segura-Bailón, B.; Lapidus, G. T. Effect of temperature on copper, iron and lead leaching from e-waste using citrate solutions. *Waste Manage.* **2018**, *71*, 420–425.

(49) Natarajan, S.; Boricha, A. B.; Bajaj, H. C. Recovery of value-added products from cathode and anode material of spent lithium-ion batteries. *Waste Manage.* **2018**, *77*, 455–465.

(50) Vander Hoogerstraete, T.; Wellens, S.; Verachtert, K.; Binnemans, K. Removal of transition metals from rare earths by solvent extraction with an undiluted phosphonium ionic liquid: separations relevant to rare-earth magnet recycling. *Green Chem.* **2013**, *15*, 919–927.

(51) Dupont, A.-L.; Têtreault, J. Cellulose Degradation in an Acetic Acid Environment. *Stud. Conserv.* **2000**, *45*, 201–210.

(52) Chung, N. H.; Tabata, M. Salting-out phase separation of the mixture of 2-propanol and water for selective extraction of cobalt(II) in the presence of manganese(II), nickel(II), and copper(II). *Hydrometallurgy* **2004**, *73*, 81–89.

(53) Nayl, A. A.; Elkhashab, R. A.; Badawy, S. M.; El-Khateeb, M. A. Acid leaching of mixed spent Li-ion batteries. *Arabian J. Chem.* **2017**, *10*, S3632–S3639.

(54) Sorint, S. S.; Jackson, L. P. Evaluation of the toxicity characteristic leaching procedure (TCLP) on utility wastes. *Nucl. Chem. Waste Manage.* **1988**, *8*, 217–223.

(55) Tipping, E.; Woof, C.; Walters, P. B.; Ohnstad, M. Conditions required for the precipitation of aluminium in acidic natural waters. *Water Res.* **1988**, *22*, 585–592.

(56) Powell, K. J.; Brown, P. L.; Byrne, R. H.; Gajda, T.; Heffer, G.; Sjöberg, S.; Wanner, H. Chemical speciation of environmentally significant metals with inorganic ligands Part 2: The Cu²⁺-OH-, Cl-, CO₃²⁻, SO₄²⁻, and PO₄³⁻ systems (IUPAC Technical Report). *Pure Appl. Chem.* **2007**, *79*, 895–950.

(57) Cognet, M.; Cambedouzou, J.; Madhavi, S.; Carboni, M.; Meyer, D. Targeted removal of aluminium and copper in Li-ion battery waste solutions by selective precipitation as valuable porous materials. *Mater. Lett.* **2020**, *268*, 127564.